

High gain multi-layered microstrip patch antenna for x- band applications

Jada Nageswara Rao^{1,2}, Ragipindi Ramana Reddy³

¹Department of ECE, JNT University Anantapuramu, Anantapur, India

²Adhoc, JNTUA College of Engineering, Pulivendula, India

³Department of ECE, JNT University Anantapuramu, Kalikiri, India

Article Info

Article history:

Received Jan 9, 2024

Revised Oct 22, 2025

Accepted Nov 5, 2025

Keywords:

High gain

High-frequency structure simulator

Multi layer

Wide band

X Band

ABSTRACT

This research investigates the development of a multi-stacked microstrip antenna featuring two patch elements positioned in a layered configuration. The antenna design incorporates three substrates with different dielectric constants, separated by an air gap, to evaluate their impact on improving bandwidth and gain. The primary objective of this research is to enhance the efficiency of a microstrip patch antenna by utilising a multilayer substrate structure. Simulation results indicate that stacking substrates with varying dielectric properties significantly enhances antenna performance. The bandwidth increases considerably, from 1.38 GHz to 2.37 GHz, while the peak gain improves from 6.6 dBi to 7.9 dBi. These advancements highlight the antenna's effectiveness in operating within the X-band frequency range, making it suitable for wireless and satellite communication systems. The design and its performance were analysed using high-frequency structure simulator (HFSS) simulation software, which validated its practical feasibility. This innovative configuration addresses the bandwidth limitations typically associated with conventional microstrip antennas, ensuring improved operational efficiency for modern communication technologies. The findings highlight the benefits of utilising a multi-stacked structure to achieve superior antenna performance, particularly in advanced communication applications.

This is an open access article under the [CC BY-SA](https://creativecommons.org/licenses/by-sa/4.0/) license.



Corresponding Author:

Jada Nageswara Rao

Department of ECE, JNT University Anantapur

Sir Mokshagundam Vishveshwariah Road, Andhra Pradesh 515002, India

Email: jadanageswararao@gmail.com

1. INTRODUCTION

Microstrip antennas have emerged as a leading choice in contemporary wireless communication systems due to their compact size, lightweight design, and ease of integration. However, the drawbacks of single-layer microstrip antennas, particularly in terms of bandwidth and radiation efficiency, have led to the exploration of more advanced antenna structures. Multilayer microstrip antennas, characterised by their stacked configuration of dielectric substrates and radiating elements, offer a promising solution to overcome these limitations. This paper aims to investigate the design, analysis, and performance of multilayer microstrip antennas in the context of next-generation communication technologies. By exploiting the advantages of multilayer structures, such as enhanced bandwidth, reduced losses, and improved radiation patterns, this research seeks to contribute to the advancement of antenna systems for applications in satellite communications, radar systems, and wireless networks.

A multilayered aperture-coupled microstrip patch antenna tailored for WLAN applications is presented. Featuring an 'I' and 'H' slot design on the ground plane, controlled by feed line length, the antenna achieves an excellent reflection coefficient, low voltage standing wave ratio (VSWR), and broadside radiation with a gain exceeding 5 dBi. The aperture-coupled stacked design demonstrated good bandwidth performance for WLAN applications; however, limited gain and lack of polarisation control reduce its effectiveness for high-performance and directional systems [1]. A wide-band stacked microstrip patch antenna is introduced in this paper. This antenna has extensive bandwidth and enhanced radiation properties, making it well-suited for X-band applications. The compact wideband multilayer antenna achieved a gain of approximately 5.23 dBi; however, the gain remains modest and could be enhanced through improved substrate tuning and material optimisation [2]. In this a stacked double-layer circular fractal microstrip antenna for X-band applications is presented. Modifications to the ground plane minimised surface wave effects, enhancing radiation efficiency. The antenna's improved impedance matching and omnidirectional radiation characteristics make it suitable for radar, mobile, and satellite communications [3]. In this work a stacked patch antenna with E-shaped and U-slot patches is discussed. It operates in the frequency spectrum of 3.27-5.85 GHz. The study examines the effect of patch separation and slot dimensions on bandwidth and impedance matching, highlighting the significance of optimal coupling for improved performance [4]. A C-type single feed for wide-band circularly polarised stacked microstrip antennas (CPSMAs), emphasising AR bandwidth and gain, is presented. The design incorporates a probe-fed stack with a parasitic patch and foam layer, with a particular focus on substrate and patch aspect-ratio adjustments. Wideband circular polarization was achieved using foam layers and a C-type feed; however, the use of foam reduces mechanical stability and adds fabrication complexity, limiting the antenna's practical deployment [5].

A wideband, compact, multi-stacked patch antenna with an average gain of 7dBi and a peak gain of 9dBi at 6.5GHz is presented. Low cross-polarisation unidirectional radiation is facilitated by the antenna's semi-circular slot and T-shaped stub [6]. The proposed H-shaped slotted multilayer stacked antenna for X-band operation exhibits wideband performance with a simulated impedance bandwidth of 2.12 GHz, and optimal efficiency is achieved at a 1.5 mm substrate gap. The antenna demonstrates high radiation efficiency with a maximum gain of 7.62 dB [7].

The stacked bow-tie slot antenna presented in the paper achieved high radiation efficiency over a wide bandwidth. The stacked bow-tie aperture antenna provided 27% bandwidth and high efficiency; however, its slot-based geometry is less suitable for printed circuit board (PCB) integration and lacks polarisation control, limiting its versatility in practical applications [8]. This work introduces a C-band dual-resonant antenna utilising FR4 and Mica substrates. It achieved significant impedance bandwidths, peak gain, and excellent cross-polarisation characteristics [9]. A broadband stacked offset microstrip antenna, which has enhanced gain and minimum cross-polarisation, is presented. The antenna achieved a maximum gain of 8.07 dBi and maintains a front-to-back ratio exceeding 12 dB. The planar monopole antenna delivered ultra-wideband (UWB) coverage with effective notch filtering; however, the absence of stacking and gain optimisation makes it unsuitable for targeted high-gain applications in the X-band [10]. A dual-feed stacked patch antenna designed for L and S bands, featuring corner-truncated probes fed by a T-shaped slot to enhance gain and axial ratio, is presented. The adjustable air gap between the ground plane and the substrate improves bandwidth and resonant frequencies, allowing for tuning and increased bandwidth. The dual-feed stacked patch antenna achieved circular polarization in L/S bands; however, its complex feeding structure and limitation to low-frequency operation restrict its applicability in compact [11].

The designed two-layer metasurface significantly reduced radar cross section (RCS) across a broad band when integrated with a single or 1×4 stacked patch array. By utilizing metallic square loops, resistors, and square metallic patches, the metasurface effectively absorbs incoming power in specific frequency bands, showcasing high absorption and minimal reflection [12]. A stacked multilayer patch and multiple-band antenna design for handheld terminals are presented. Utilizing corner truncation and I-slot, the antenna enhances radiation efficiency [13]. A circularly polarised aperture stacking patch (ASP) antenna is introduced, utilising four parasitic patches rotated by 30° to achieve AR <3dB and VSWR <2. It offers a bandwidth of 33.6% in a single element and 36.15% in a 2×1 array [14].

A low-cost, high-gain, broadband stacked multi-layer triangular microstrip antenna (ETMSA) has been developed for the 1,700-2,600 MHz frequency range, with a focus on minimising cross-polarisation. The antenna includes a metallic via for cross-polarisation enhancement and a metallic cavity for gain improvement. It offers a bandwidth of 42.2%, a peak gain of 10.8 dBi, an over 15.8 dB front-to-back ratio, and less than -13.6 dB cross-polarisation, making it suitable for RF energy harvesting in various bands. The use of parasitic triangular patches and a cavity structure enabled high gain, but the complex geometry and restriction to lower frequency bands limit its suitability for compact and higher-band applications [15]. A square patch antenna featuring pentagon and hexagon slots, augmented by a rectangular defected ground structure (DGS), is tailored for 5G and LTE applications. The inclusion of DGS significantly boosts the

antenna's performance, offering a wider bandwidth and improved return loss [16]. A dual-polarised stacked patch antenna with wideband capabilities, addressing the needs of modern wireless communication systems, is presented. The antenna prototype demonstrated excellent performance in terms of impedance matching and isolation [17]. The research paper presented a comprehensive study on a stacked patch design for broad impedance bandwidth, axial-ratio (AR) bandwidth and flat gains, offering a significant contribution to the field of antenna engineering. Flat gain and wide AR bandwidth were achieved using stacked patches and a loop feed; however, the use of vertical parasitic walls and complex feeding increases structural complexity [18]. The proposed modified U-slot stacked multilayer antenna for UWB applications demonstrates a significant improvement over conventional microstrip patch antennas. UWB operation was achieved using a modified U-slot stacked patch; however, the design lacks control over radiation direction and offers limited gain [19]. A paper on the broadband stacked strip antenna design for X-band applications, operating with a bandwidth of more than 4 GHz, which corresponds to approximately 42% of the centre frequency, is presented [20].

In this paper, design of a multiple-layer double U-slot microstrip patch antenna is presented. Incorporating three layers into the antenna structure enhanced the bandwidth, resulting in broader frequency coverage [21]. A stacked rectangular strip antenna with an inset feeding mechanism is designed and implemented. It consists of a microstrip patch that operates at 10 GHz and a 9×9 electromagnetic bandgap (EBG) array on a 0.5 mm-thick FR-4 epoxy substrate. It achieved a minimum reflectivity of -30.57 dB at 9.9 GHz and a gain of 9.45 dBi across both the E and H planes with a -10 dB reflection bandwidth of 1.2 GHz [22]. A 3D-printed multilayer stacked microstrip patch array (SMPA) antenna for ISM band applications operating in the 2.4-2.5GHz frequency range is presented. Based on experimental results, the SMPA antenna is ideal for ISM band communication applications since it has a modest gain of 10-11 dBi [23]. The stacked patch antenna with crossed slots presented in the research paper offers acceptable impedance matching at the ports over a large bandwidth, ensuring a good gain performance. The measured return loss demonstrates acceptable bandwidth performance and low back radiation, indicating excellent antenna performance [24]. A Hexagonal patch antenna with pentagon and hexagon-shaped slots, along with a rectangular DGS, is designed for 5G and LTE applications. The use of DGS greatly enhances the antenna's performance by increasing bandwidth and improving return loss [25]. In this article, a multi-layered antenna is presented. The impact of multiple substrates on the gain and bandwidth is analysed. The antenna is simulated using the high-frequency structure simulator (HFSS) software.

2. ANTENNA DESIGN

Figure 1 illustrates the configuration of the suggested antenna. The proposed antenna design was developed and analyzed using Ansys HFSS 2021 simulation software, employing the finite element method (FEM) for accurate electromagnetic analysis. The methodology involved a systematic phase-wise evolution of the antenna structure, starting from a basic rectangular microstrip patch and progressing through aperture-coupled, multi-substrate, and stacked configurations. Each phase was simulated to evaluate the effects of substrate material, patch dimensions, and the introduction of an air gap. This antenna element comprises three layers of dielectric substrates along with an air gap layer. The initial layer is composed of FR4 Epoxy, characterised by a dielectric constant of 4.4 and a height of 1.6 mm, which serves as the antenna. The second layer consists of an Arlon AD250A™ substrate, which has a height of 0.25 mm and a dielectric constant of 2.50. This is succeeded by an RT/Duroid®5880 layer, exhibiting a dielectric constant of 2.2 and a thickness of 1.5 mm; this is utilised for the patch two-layer. Between the second and third layers, introduce an air gap with a thickness of 1.2 mm, aimed at enhancing the operational bandwidth and gain of the antenna. The measurements of the suggested antenna are detailed in Table 1, and Figure 2 shows the top view of the proposed antenna.

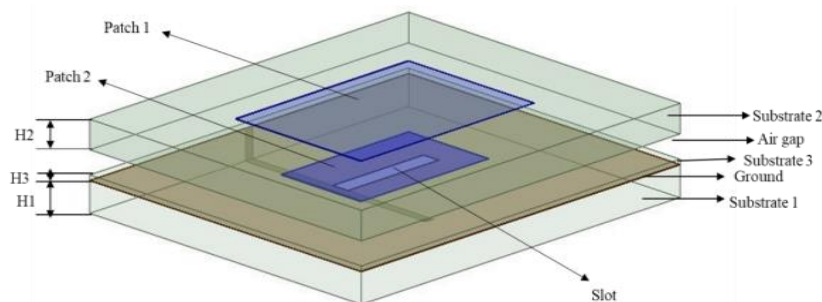


Figure 1. Geometry of the suggested antenna

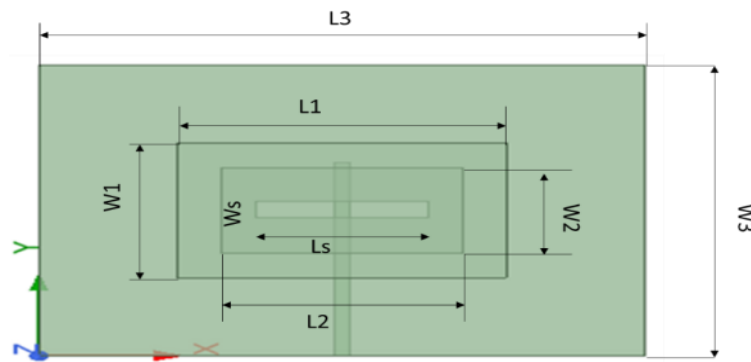


Figure 2. Top view of the proposed antenna

Table 1. Dimensions of the suggested antenna

| Parameter | L ₁ | W ₁ | L ₂ | W ₂ | L ₃ | W ₃ | H ₁ | H ₂ | H ₃ | L _S | W _S | Air gap |
|-----------------|----------------|----------------|----------------|----------------|----------------|----------------|----------------|----------------|----------------|----------------|----------------|---------|
| Dimensions (mm) | 11.4 | 8.28 | 8.4 | 5.28 | 21 | 17.88 | 1.6 | 1.5 | 0.25 | 6 | 1 | 1.2 |

The antenna consists of three substrates: FR4-epoxy ($\epsilon_r = 4.4$), Arlon AD250A ($\epsilon_r = 2.5$), and RT/Duroid® 5880 ($\epsilon_r = 2.2$), with a 1.2 mm air gap between the second and third layers to improve bandwidth and gain. Key simulation parameters such as return loss (S11), gain, and radiation patterns were extracted. Parametric studies were also performed to optimise substrate thickness and patch dimensions for best performance. The results of each phase were compared to quantify the improvements achieved at each design stage.

2.1. Evolution of proposed antenna

The initial rectangular microstrip patch antenna (RPA) was created utilising the following design parameters: patch length (L), patch width (W), and feed location from the centre of the patch. The following design equations were used to estimate length and width: $f = 8$ GHz, $\epsilon_r = 4.4$ and $h = 1.6$ mm.

$$W = \frac{c}{2f\sqrt{\frac{\epsilon r + 1}{2}}} \quad (1)$$

$$L = \frac{c}{2f} \left(\frac{\varepsilon r + 1}{2} + \frac{\varepsilon r - 1}{2} \sqrt{1 + 12 \frac{h}{w}} \right)^{-1/2} \quad (2)$$

The speed of light, denoted as 'c', is considered to be 3×10^8 m/s. Upon substitution, the dimensions of the patch were determined as a width (W) of 8.28 mm and a length (L) of 11.4 mm. Using (1) and (2), a rectangular patch antenna is designed as shown in Figure 3. The substrate is FR4 Epoxy with a height of 1.6 mm, a dielectric constant of $\epsilon_r = 4.4$, and a loss tangent value of 0.0001. The simulation results for the rectangular patch show a return loss of -13.10 dB and a gain of 5.93 dBi.

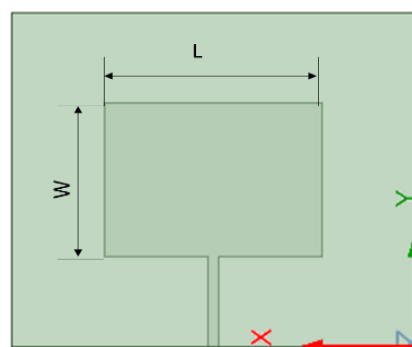


Figure 3. Rectangular patch antenna

The proposed antenna design process involves four distinct phases as follows,

– Phase 1: Aperture-coupled rectangular patch antenna (ACA)

An ACA is created using a sandwiched ground with a rectangular slot positioned between substrates 1 and 2, as illustrated in Figure 4. Substrate 1 is utilised for the feed line, while substrate two supports radiating patch 1, forming a basic aperture-coupled microstrip antenna. The electric field distribution in this configuration is primarily concentrated around the aperture slot and underneath Patch 1, indicating a fundamental level of coupling between the feed and the patch through the slot as shown in Figure 4. However, due to the relatively simple structure and single radiating patch, the gain remains limited and the energy confinement is moderate. Despite these constraints, the configuration achieves significant improvements over traditional microstrip antennas. While conventional designs typically operate with narrow bandwidths in the megahertz range, this aperture-coupled antenna attains a much broader bandwidth of 1.38 GHz, as shown in Figure 5. Additionally, it exhibits two resonant peaks at 8.6 GHz and 9.44 GHz, with return losses of -20.49 dB and -17.22 dB, respectively. Figure 6 illustrates the E-field plot, which further supports these results by showing localised energy concentration, which motivates further structural enhancements in subsequent design phases to improve field distribution, bandwidth, and gain.

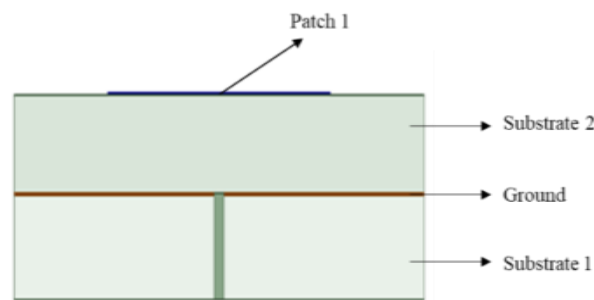


Figure 4. Side view of ACA

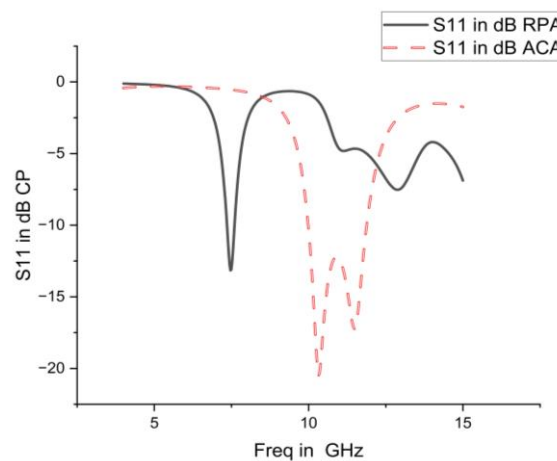


Figure 5. S11 parameter plot of RPA and ACA

– Phase 2: ACA with additional substrate (ACAS)

In this phase, substrate 3 is introduced between the ground plane and substrate 2, resulting in an ACA with an additional substrate (ACAS), as shown in Figure 7. This modification creates a more layered structure, influencing the electromagnetic behaviour of the antenna. A parametric analysis is conducted on the dimensions and thickness of substrate 3. Altering its dimensions results in consistent gain and bandwidth, with minor shifts in resonant frequencies. Changes in the thickness are effecting both the bandwidth and gain. At a thickness of 0.25 mm, the bandwidth is 1.29 GHz, with gains of 6.1 dBi and 6.5 dBi at 8.6 GHz and 9.28 GHz, respectively. Increasing the thickness to 0.5 mm yields a 1.24 GHz bandwidth, with gains of 6.2 dBi and 6.4 dBi at 8.68 GHz and 9.2 GHz, respectively. Further increasing thickness to 0.75 mm reduces the

bandwidth to 1.05 GHz, with a gain of 6.2 dBi at 8.94 GHz. These observations indicate that increasing the thickness of substrate 3 decreases bandwidth. Therefore, among the variations, the thinnest thickness (0.25 mm) is selected, producing return losses of -26.0 dB at 8.68 GHz and -24.11 dB at 9.26 GHz, with gains of 6.1 and 6.5 dBi at 8.6 GHz and 9.28 GHz, respectively.

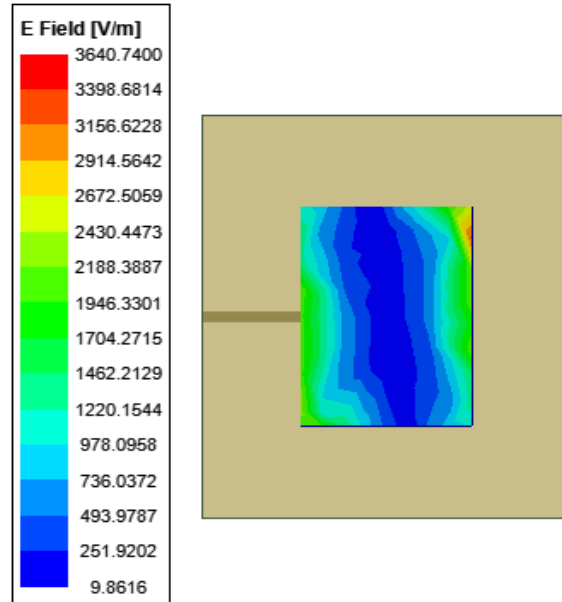


Figure 6. E-Field distribution of ACA

The improved performance in this phase is also evident from the E-field distribution, which shows increased field intensity and a broader spread across the stacked dielectric layers as shown in Figure 8. The inclusion of Substrate 3 enhances the effective dielectric height and enables stronger confinement of electromagnetic fields. This, in turn, leads to better impedance matching and facilitates the excitation of additional resonant modes through improved energy transfer via the aperture. Compared to Phase 1, the E-field plots confirm a more efficient field propagation and distribution, correlating directly with the observed improvements in gain and bandwidth.

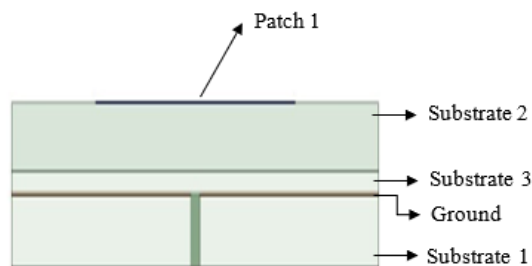


Figure 7. Side view of ACAS

– Phase 3: ACA with additional substrate and patch (ACASP)

In this phase, a patch is added above the substrate, resulting in an ACA with additional substrate and patch (ACASP) as illustrated in Figure 9. This structural enhancement creates a stacked patch configuration, which significantly influences the antenna's electromagnetic behaviour and performance. Parametric analysis is done on its length and width. Considering the same dimensions as patch 1 resulted in a single resonant peak at 7.88 GHz, a bandwidth of 10 MHz and a gain of 5.7 dBi at 7.88 GHz. At dimensions of 8.24 mm in length and 5.28 mm in width, the bandwidth reaches 1.4 GHz, with gains of 6.0 dB and 6.3 dB at 8.56 GHz

and 9.4 GHz, respectively. A further reduction to 7.24 mm length and 4.28 mm width results in a bandwidth of 1.34 GHz and gains of 6.1 and 6.4 at 8.62 GHz and 9.32 GHz, respectively. Based on these observations, the optimal dimensions are determined to be 8.24 mm and 5.28 mm, producing a multi-band configuration with three resonant peaks. The return losses obtained are -21.96 dB, -18.0 dB, and -26.62 dB at frequencies of 8.56 GHz, 9.4 GHz, and 11.7 GHz, respectively, encompassing a bandwidth of 1.4 GHz. The improvement in performance is further confirmed by the electric field distribution, which reveals strong E-field intensities at both Patch 1 and Patch 2, as shown in Figure 10. This indicates effective mutual coupling between the patches, leading to the excitation of multiple closely spaced resonant modes and enhanced energy distribution. The stacking also increases the effective radiating aperture, improving gain and radiation efficiency. The E-field plots clearly demonstrate a more uniform and intense field distribution compared to previous phases, validating the effectiveness of the stacked configuration in significantly enhancing both bandwidth and gain.

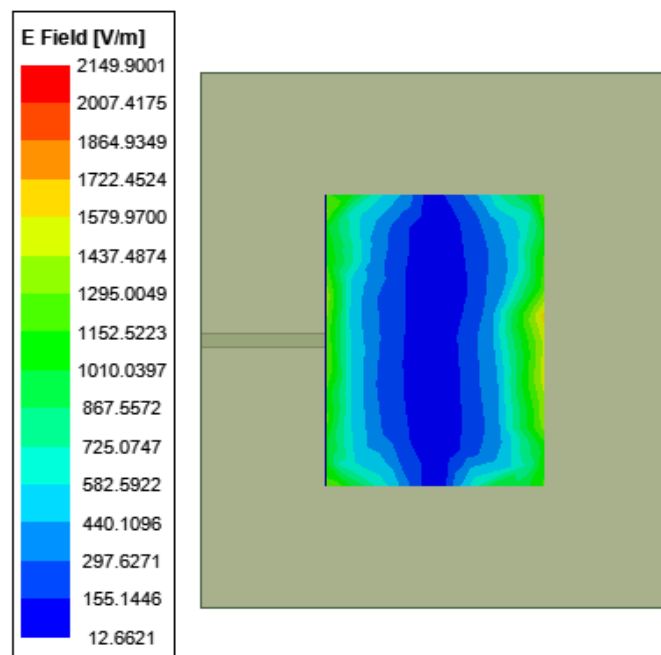


Figure 8. E-field distribution of ACAS

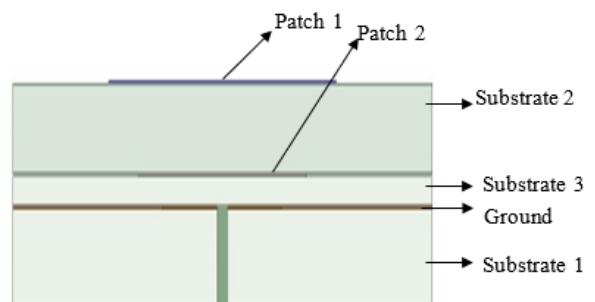


Figure 9. Side view of ACASP

- Phase 4: ACA with additional substrate, patch and air gap (ACASPA)

In this phase, an air gap is introduced between patch two and substrate two, resulting in an ACA with an additional substrate, patch, and air gap (ACASPA), as shown in Figure 11. This modification significantly impacts the antenna's dielectric environment and electromagnetic performance. Parametric analysis is done on the thickness of the air gap. At 0.9 mm thickness, the configuration yielded a 1.62 GHz

bandwidth, with gains of 6.5 dBi and 7.37 dBi at 8.9 GHz and 9.66 GHz, respectively. At 1 mm thickness, the configuration yielded a 1.59 GHz bandwidth and gains of 6.5 dBi and 7.4 dBi at 8.92 GHz and 9.62 GHz, respectively. With 1.2 mm thickness, the configuration resulted in a 2.37 GHz bandwidth with gains of 6.6 dBi, 7.5 dBi, and 7.9 dBi at 8.92 GHz, 9.62 GHz, and 10.8 GHz, respectively. Further, by increasing the thickness, the bandwidth is reduced. The 1.2 mm air gap thickness is ultimately selected. The return loss at the specified peaks is recorded at -16.75 dB, -15.32 dB, and -17.96 dB for frequencies of 8.94 GHz, 9.56 GHz, and 10.8 GHz, respectively, yielding an overall bandwidth of 2.37 GHz. Gains of 6.6 dBi, 7.5 dBi, and 7.9 dBi are observed at 8.94 GHz, 9.56 GHz, and 10.8 GHz, respectively. This design gives favourable radiation patterns and directivity. The radiation pattern plot consists of both E-field and H-field patterns. The E-field plots further validate the design, showing a highly uniform and intense electric field distribution, particularly concentrated around Patch 2 as shown in Figure 12. This indicates enhanced radiation efficiency and reduced dielectric losses due to the lower effective permittivity introduced by the air gap. Moreover, the air gap provides better control over surface currents and improves impedance matching, which contributes directly to the antenna achieving its highest overall gain and widest bandwidth in this phase. The combined effects of optimised field distribution, minimised substrate loading, and improved dielectric transition establish this configuration as the most efficient and high-performing design among all four phases.

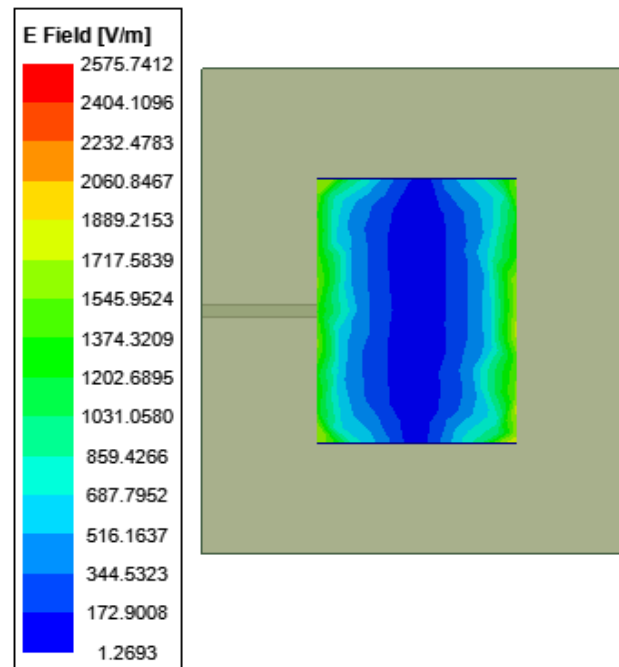


Figure 10. E-Field distribution of ACASP

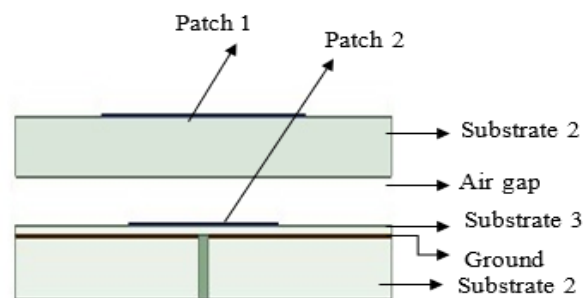


Figure 11. Side view of ACASP

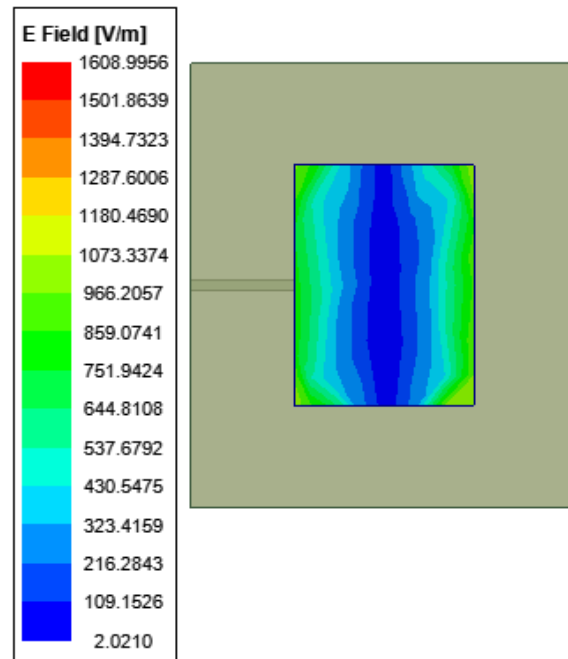


Figure 12. E-field distribution of ACASP

3. RESULTS AND DISCUSSION

From the simulation results presented in Figure 13, the presented antenna is offering a bandwidth of 2.37 GHz, ranging from 8.65 GHz to 11.02 GHz. The results section has been enriched with comprehensive numerical analysis and performance evaluation across all design phases. Phase-wise comparisons clearly demonstrate the progressive improvements in bandwidth and gain achieved through multilayer stacking and the introduction of an optimised air gap. The final antenna configuration achieved a wide impedance bandwidth of 2.37 GHz, covering the range from 8.65 GHz to 11.02 GHz, with three distinct resonant peaks. Corresponding return loss values of -16.85 dB, -15.32 dB, and -17.96 dB validate effective impedance matching. Peak gain values of 6.6 dBi, 7.5 dBi, and 7.9 dBi were recorded at 8.94 GHz, 9.56 GHz, and 10.8 GHz, respectively as shown in Figures 17(a)-(c). These values have been tabulated and compared with other state-of-the-art designs, showing that the proposed design offers superior bandwidth while maintaining competitive gain levels, confirming its effectiveness for high-performance X-band applications. Figures 14 to 18 display the simulated radiation patterns, gain and directivity plots of the suggested antenna.

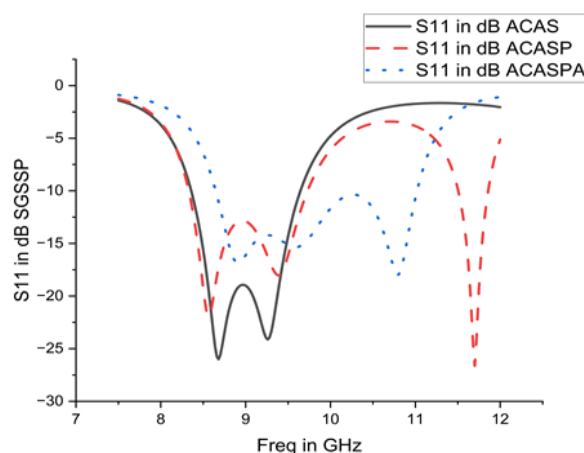


Figure 13. Comparison of the return loss obtained from Phase 2 to Phase 4

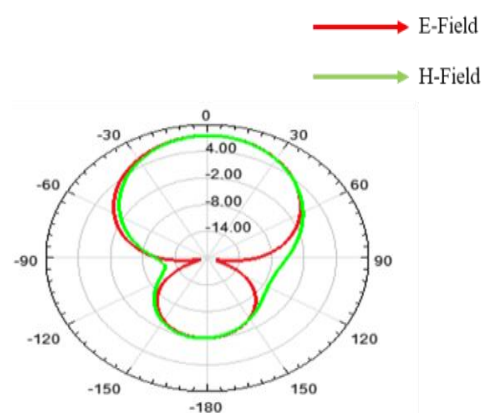


Figure 14. E-field and H-field pattern of ACASP at 8.94 GHz

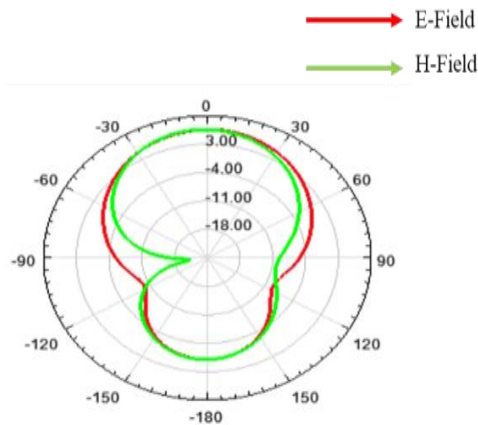


Figure 15. E-field and H-field pattern of ACASP at 9.56 GHz

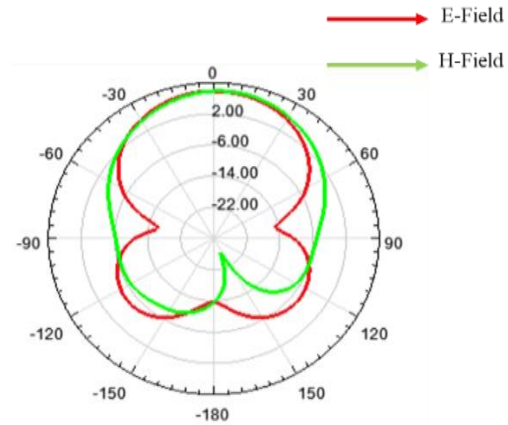


Figure 16. E-field and H-field pattern of ACASP at 10.8 GHz

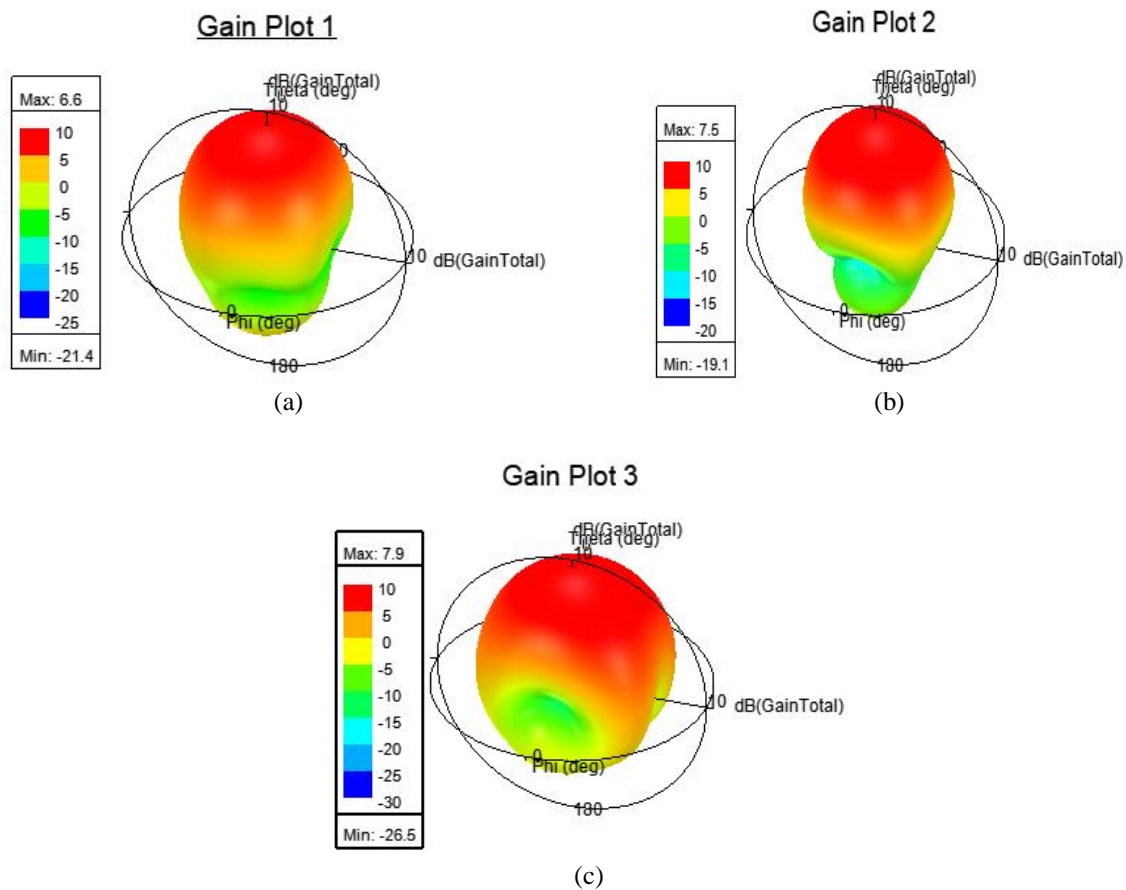


Figure 17. Gain plot of the presented antenna at (a) 8.94 GHz, (b) 9.56 GHz and (c) 10.8 GHz

The proposed high-gain, wideband multilayer microstrip patch antenna is particularly suitable for a variety of X-band applications. Given its enhanced bandwidth of 2.37 GHz and peak gain of up to 7.9 dBi as shown in Figure 17(c), the antenna can be effectively utilised in satellite uplinks, radar front-end modules, airborne communication systems, and high-speed point-to-point wireless links. The improved radiation performance and directional characteristics make it ideal for integration into systems requiring reliable high-frequency signal transmission with minimal losses. Its multilayer structure with an air gap also offers

mechanical adaptability, supporting advanced applications like synthetic aperture radar (SAR) and ground-penetrating radar (GPR) where compact, efficient, and high-performance antennas are critical. A comparison of the suggested multi-layer antenna phase-wise simulation results is presented in Table 2.

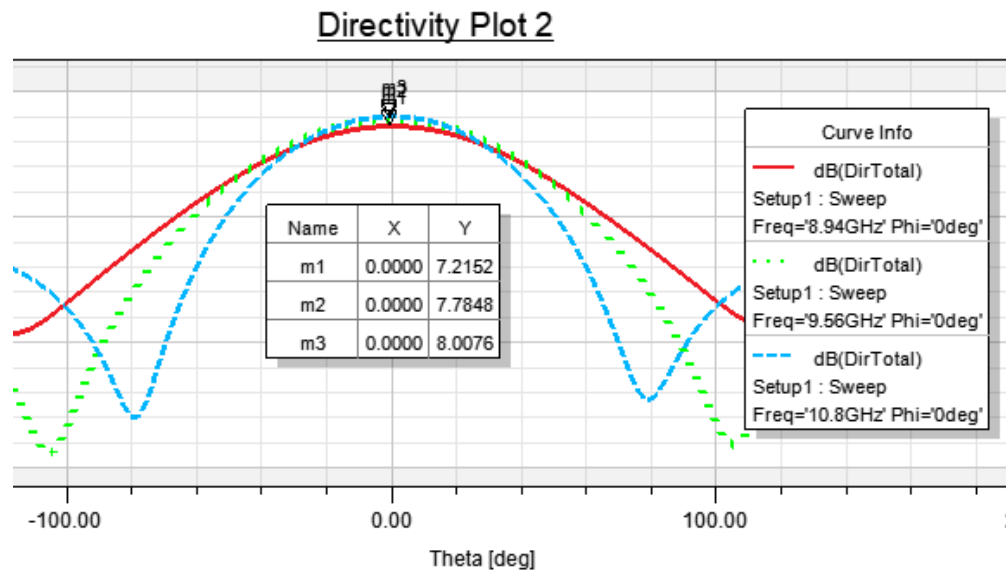


Figure 18. Directivity of the recommended antenna at different peaks

Table 2. Comparison of the phase-wise results of the proposed antenna

| Evolution | Resonant frequency (GHz) | Return loss(dB) | Bandwidth (GHz) | Peak gain(dBi) |
|-----------|--------------------------|------------------------|-----------------|----------------|
| Phase 1 | 8.62, 9.44 | -20.33, -17.22 | 1.38 | 6.0, 6.6 |
| Phase 2 | 8.6, 9.28 | -51.64, -19.15 | 1.29 | 6.1, 6.5 |
| Phase 3 | 8.56, 9.4, 11.7 | -21.96, -18, -26.62 | 1.40 | 6.0, 6.3, 6.1 |
| Phase 4 | 8.92, 9.62, 10.8 | -16.85, -19.15, -17.96 | 2.37 | 6.6, 7.5, 7.9 |

Comparison of works reported in open literature and the recommended work is presented in Table 3. Work reported in references [20]-[21] demonstrates a higher gain, which is attributed to inset feeding; however, they exhibit a narrower bandwidth. In contrast, the proposed antenna offers a wide bandwidth with high peak gain.

Table 3. Comparison of different multi-layer antennas

| Reference | Resonant frequency (GHz) | Bandwidth (GHz) | Peak gain (dBi) | Feeding Technique |
|---------------|--------------------------|-----------------|-----------------|-------------------|
| [1] | 2.51 | 0.7 | 4.091 | Aperture coupling |
| [2] | 10 | 3 | 5.23 | Aperture coupling |
| [5] | 5.7 | 1.13 | 7.5 | Co-axial feeding |
| [7] | 10.3 | 2.12 | 7.62 | Inset feeding |
| [11] | 2.480 | 0.8 | 3.6 | Probe feeding |
| [20] | 9.75 | 1.2 | 9.45 | Inset feeding |
| [21] | 2.4 | 0.6 | 10 | Inset feeding |
| [22] | 9.6 | 2 | 7 | Aperture coupling |
| Proposed work | 10.8 | 2.37 | 7.9 | Aperture coupling |

4. CONCLUSION

In this paper, a multi-layered microstrip antenna is presented. The proposed antenna is designed with three substrates along with an air gap and two patches. With multiple substrates of different dielectric constants, one above the other, the antenna bandwidth is increased from 1.38 GHz to 2.37 GHz and the peak gain is improved from 6.6 dBi to 7.9 dBi. The thickness of the proposed antenna (4.6 mm) is the limitation of this work, which can be overcome with a new 3D printing technique. Attempts will be made to reduce the thickness of the antenna in future work, maintaining or improving the bandwidth and gain.

FUNDING INFORMATION

Authors state no funding involved.

AUTHOR CONTRIBUTIONS STATEMENT

This journal uses the Contributor Roles Taxonomy (CRediT) to recognize individual author contributions, reduce authorship disputes, and facilitate collaboration.

| Name of Author | C | M | So | Va | Fo | I | R | D | O | E | Vi | Su | P | Fu |
|------------------------|---|---|----|----|----|---|---|---|---|---|----|----|---|----|
| Jada Nageswara Rao | ✓ | ✓ | ✓ | | ✓ | ✓ | | ✓ | ✓ | | | | | |
| Ragipindi Ramana Reddy | | | | ✓ | | | ✓ | ✓ | ✓ | ✓ | ✓ | ✓ | ✓ | |

C : Conceptualization

M : Methodology

So : Software

Va : Validation

Fo : Formal analysis

I : Investigation

R : Resources

D : Data Curation

O : Writing - Original Draft

E : Writing - Review & Editing

Vi : Visualization

Su : Supervision

P : Project administration

Fu : Funding acquisition

CONFLICT OF INTEREST STATEMENT

Authors state no conflict of interest.

DATA AVAILABILITY

Data availability is not applicable to this paper as no new data were created or analyzed in this study.




REFERENCES

- [1] P. Jothilakshmi, J. Bharanitharan, and V. Ramkumar, "Design of multilayer aperture coupled stacked microstrip patch antenna for wlan applications," *ICTACT Journal on Communication Technology*, vol. 6, no. 2, pp. 1105–1111, 2015, doi: 10.21917/ijct.2015.0161.
- [2] S. Lakrit and H. Ammor, "Design on X-band wideband and high-gain multi-layer microstrip antenna," *Journal of Engineering Science and Technology Review*, vol. 7, no. 3, pp. 176–179, 2014, doi: 10.25103/jestr.073.28.
- [3] J. Padhi, A. Behera, and M. Dash, "Design of a stacked two layer circular fractal microstrip antenna for X-band application," *2016 IEEE Annual India Conference, INDICON 2016*, 2017, doi: 10.1109/INDICON.2016.7839155.
- [4] M. A. Matin, B. S. Sharif, and C. C. Tsimenidis, "Probe fed stacked patch antenna for wideband applications," *IEEE Transactions on Antennas and Propagation*, vol. 55, no. 8, pp. 2385–2388, 2007, doi: 10.1109/TAP.2007.901924.
- [5] Nasimuddin, K. P. Esselle, and A. K. Verma, "Wideband circularly polarized stacked microstrip antennas," *IEEE Antennas and Wireless Propagation Letters*, vol. 6, pp. 21–24, 2007, doi: 10.1109/LAWP.2006.890749.
- [6] Parthasarathy, A. Chandrasekar, and P. G. V. Ramesh, "A compact wide band multi-stacked patch antenna for UWB applications," *Proceedings of the 2019 TEQIP - III Sponsored International Conference on Microwave Integrated Circuits, Photonics and Wireless Networks, IMICPW 2019*, pp. 77–80, 2019, doi: 10.1109/IMICPW.2019.8933207.
- [7] A. Anand and P. Suraj, "Design of a stacked microstrip patch antenna for X-band communication," *Proceedings of the 4th IEEE International Conference on Recent Advances in Information Technology, RAIT 2018*, pp. 1–5, 2018, doi: 10.1109/RAIT.2018.8389017.
- [8] C. Locker and T. F. Eibert, "Unidirectional radiation efficient stacked aperture antenna for X-B and application," *IEEE Antennas and Wireless Propagation Letters*, vol. 7, pp. 264–266, 2008, doi: 10.1109/LAWP.2008.921323.
- [9] A. Kandwal, J. V. Chauhan, and B. Luadang, "Coupled C-band stacked antenna using different dielectric constant substrates for communication systems," *Engineering Science and Technology, an International Journal*, vol. 19, no. 4, pp. 1801–1807, 2016, doi: 10.1016/j.jestch.2016.08.005.
- [10] V. P. Sarin, M. S. Nishamol, D. Tony, C. K. Aanandan, P. Mohanan, and K. Vasudevan, "A wideband stacked offset microstrip antenna with improved gain and low cross polarization," *IEEE Transactions on Antennas and Propagation*, vol. 59, no. 4, pp. 1376–1379, 2011, doi: 10.1109/TAP.2011.2109362.
- [11] D. H. Dabhi and M. A. Ardeshana, "Dual feed stacked patch antenna for L and S band application," *Proceedings of the 2nd International Conference on Trends in Electronics and Informatics, ICOEI 2018*, pp. 256–259, 2018, doi: 10.1109/ICOEI.2018.8553939.
- [12] C. Huang, W. Pan, X. Ma, and X. Luo, "Wideband radar cross-section reduction of a stacked patch array antenna using metasurface," *IEEE Antennas and Wireless Propagation Letters*, vol. 14, pp. 1369–1372, 2015, doi: 10.1109/LAWP.2015.2407375.
- [13] O. P. Falade, Y. Gao, X. Chen, and C. Parini, "Stacked-patch dual-polarized antenna for triple-band handheld terminals," *IEEE Antennas and Wireless Propagation Letters*, vol. 12, pp. 202–205, 2013, doi: 10.1109/LAWP.2013.2245392.
- [14] H. Oraizi and R. Pazoki, "Wideband circularly polarized aperture-fed rotated stacked patch antenna," *IEEE Transactions on Antennas and Propagation*, vol. 61, no. 3, pp. 1048–1054, Mar. 2013, doi: 10.1109/TAP.2012.2229378.
- [15] R. Chopra and G. Kumar, "High gain broadband stacked triangular microstrip antennas," *Microwave and Optical Technology Letters*, vol. 62, no. 9, pp. 2881–2888, 2020, doi: 10.1002/mop.32372.
- [16] J. N. Rao, M. S. Chandana, R. R. Reddy, and K. Sainath, "Effect of DGS on slotted square patch antenna for 5G and LTE applications," *2024 IEEE Wireless Antenna and Microwave Symposium, WAMS 2024*, 2024, doi: 10.1109/WAMS59642.2024.10528047.




- [17] A. A. Serra, P. Nepa, G. Manara, G. Tribellini, and S. Cioci, "A wide-band dual-polarized stacked patch antenna," *IEEE Antennas and Wireless Propagation Letters*, vol. 6, pp. 141–143, 2007, doi: 10.1109/LAWP.2007.893101.
- [18] K. Ding, Y. Wu, K. H. Wen, D. L. Wu, and J. F. Li, "A stacked patch antenna with broadband circular polarization and flat gains," *IEEE Access*, vol. 9, pp. 30275–30282, 2021, doi: 10.1109/ACCESS.2021.3059948.
- [19] M. Surana and A. K. Jain, "Modified U-slot stacked micro-strip patch antenna for ultra- wideband applications in S band, C band and X band," *Journal of Applied and Computational Mechanics*, vol. 3, no. 4, pp. 293–301, 2017, doi: 10.22055/jacm.2017.12638.
- [20] C. Schulz, C. Baer, T. Musch, and I. Rolfes, "A broadband stacked patch antenna with enhanced antenna gain by an optimized ellipsoidal reflector for X-band applications," *2011 IEEE International Conference on Microwaves, Communications, Antennas and Electronic Systems, COMCAS 2011*, 2011, doi: 10.1109/COMCAS.2011.6105928.
- [21] N. K. Darimireddy, R. Ramana Reddy, and A. Mallikarjuna Prasad, "Design of triple-layer double U-slot patch antenna for wireless applications," *Journal of Applied Research and Technology*, vol. 13, no. 5, pp. 526–534, 2015, doi: 10.1016/j.jart.2015.10.006.
- [22] M. Gaharwar and D. C. Dhubkary, "X-band multilayer stacked microstrip antenna using novel electromagnetic band-gap structures," *IETE Journal of Research*, vol. 69, no. 4, pp. 2015–2024, 2023, doi: 10.1080/03772063.2021.1883484.
- [23] M. A. Belen, "Stacked microstrip patch antenna design for ISM band applications with 3D-printing technology," *Microwave and Optical Technology Letters*, vol. 61, no. 3, pp. 709–712, 2019, doi: 10.1002/mop.31603.
- [24] F. Klefenz and A. Dreher, "Aperture-coupled stacked microstrip antenna with dual polarization and low back-radiation for X-band SAR applications," pp. 179–182, 2002, doi: 10.1109/rawcon.2000.881884.
- [25] A. R. Banyan, V. Pravallika, J. N. Rao, R. R. Reddy, and D. S. Rani, "Hexagonal patch antenna with slots and DGS for S and C band applications," *2024 IEEE Wireless Antenna and Microwave Symposium, WAMS 2024*, 2024, doi: 10.1109/WAMS59642.2024.10528032.

BIOGRAPHIES OF AUTHORS



Jada Nageswara Rao    received M. Tech in 2016 from MITS, Madanapalle. Presently pursuing Ph.D. from JNTUA. He is working as Assistant Professor (Adhoc) in Dept. of ECE, JNTUA College of Engineering Pulivendula from 2017. He published 10 technical papers in various Journals and Conferences of repute. His research interests include microwave antennas and array antennas. He can be contacted at email: jadanageswararao@gmail.com.



Dr. Ragipindi Ramana Reddy    done M.Tech (I&CS) in 2002 from JNTUK, Kakinada, MBA from AU in 2007 and Ph.D. in 2008 in Antennas from AUCE(A), AU. Presently Professor, Dept. of ECE, JNTUACEK. Chairman, BoS, ECE, JNTUA Anantapur. Former Principal, JNTUACEP. Published 160 technical papers in International/National Journals and Conferences. 05 Patents granted. Reviewer of IEEE A&P Transactions, Letters and Magazine. Senior Member of IEEE, FIETE, FIE, and MISTE. His research interests include Antennas, EMI/EMC, VLSI and Embedded Systems. He can be contacted at email: rreddy.ece@jntua.ac.in.